Effect of charge transfer band on luminescence properties of Yb doped Y_2O_3 nanoparticles

Pratik Deshmukh, S. Satapathy*, Anju Ahlawat, Khemchand Sahoo, P. K. Gupta

Nano Functional Materials Laboratory, Laser Materials Development & Devices Division, Raja Ramanna Centre for Advanced Technology, Indore 452013, India

*Corresponding author, Tel: (+91) 731 2488660/8658; Fax: (+91) 731 2488650; E-mail: srinu73@cat.ernet.in, srinusatapathy@gmail.com

Received: 20 March 2016, Revised: 04 July 2016 and Accepted: 13 October 2016

DOI: 10.5185/amlett.2017.6560
www.vbripress.com/aml

Abstract

The photoluminescence properties of Yb doped Y_2O_3 nanoparticles were investigated in visible region to resolve the origin of dissimilar fluorescence peaks at different excited wavelengths and to explore possible use of Yb: Y_2O_3 for white light emission, excited by available near UV LED. The peak observed at 370 nm in photoluminescence excitation spectrum is due to expected transition of electrons from $^2F_{7/2}$ to charge transfer band (CTB) associated with non-centrosymmetric C_2 centers however, the excitation peak at 335 nm is due to transition of electrons from $^2F_{7/2}$ to the CTB associated with distorted centrosymmetric C_{3i} centers. The Yb doping in nano Y_2O_3 not only modify the CTB but also helps in transition of electron from these CTBs to ground $^2F_{5/2}$ and $^2F_{7/2}$ levels of Yb. Strong broad emission peak is observed at 503 nm which is assigned to transition from distorted CTB (C_{3i}) to $^2F_{5/2}$ energy levels. The findings are important because broad emission (from ~400 to ~650 nm) at 335 nm excitation (available AlGaN LED wavelength) due to C_2 and C_{3i} centers in Yb: Y_2O_3 may be used for white light emission applications. Copyright © 2017 VBRI Press.

Keywords: Photoluminescence, nanophosphor, Yb: Y_2O_3, charge transfer band, TEM.

Introduction

Charge transfer bands (CTB) are observed in several rare-earth (RE) oxide compounds and these are formed due to the transfer of electronic charge from the highest occupied orbital of the valence band in the host lattice, i. e. from the 2p orbitals of oxygen in the case of oxygen based hosts, to RE ions [**1**, **2**]. The CTB transitions are usually observed as strong and broad absorption bands in the UV-visible region as they are not restricted by any selection rules [**1**]. The CTBs in Eu^{2+} doped Sr_2SiO_4 and Eu^{2+} doped Sr_3SiO_5 phosphors play an important role in photoluminescence (PL) process for wide range emission in visible region, make these materials suitable for white light emitting diodes [**3-5**]. The part of CTB absorption energy due to Eu^{2+} in Sr (I) site transfer to Tb^{3+} ion at Sr(II) site and consequently broad luminescence from both Eu^{2+} and Tb^{3+} is observed in Eu^{2+} and Tb^{3+} doped $(Sr,Ba)_2SiO_4$ [**6**]. The broad emission in Sr_2SiO_4: Eu^{2+} is associated with ligand (oxygen) distribution around two types of Sr sites (nine coordination Sr(I) site and ten coordination Sr(II) site). Similarly, the rare earth doped Y_2O_3 is prone to CTB formation due to oxygen ligand environment around Y^{3+} ions. The Y_2O_3 as a promising optical material has excellent physical and chemical properties, such as high melting point (2430 ºC), broad range of transparency (~ 0.2 - 8 μm) and high corrosion resistance. The Y_2O_3 has a cubic crystal structure with space group Ia3 and density of 5.04 g/cm^3 with refractive index ~1.9 at 1 μm wavelength [**7**, **8**]. Due to its high effective atomic number and high density, i.e., 35 and 4.56 g cm^{-3}, respectively, Y_2O_3 can be a more effective scintillator than Yttrium aluminum garnet (YAG) [**9**].

In cubic Y_2O_3 the Y^{3+} ion occupies 24 noncentrosymmetric (C_2) and 8 centrosymmetric (C_{3i}) sites in an elementary cell. The luminescence of the Y_2O_3 is predominantly connected with noncentrosymmetric (C_2) site. Since C_{3i} site has an inversion centre, according to the selection rules electric dipole transitions are not allowed for ions occupying this site, because these sites cannot provide odd terms in the crystal field [**10**]. Y_2O_3 crystallizes in monoclinic phase (space group C2/m) and possesses three crystallographically distinct cation sites with seven-fold coordination, each having point group symmetry C_s [**11**]. However, Y_2O_3 crystallizes in cubic phase in majority of synthesis method. The C_2 and C_{3i} cation sites associated with two different centers of distorted octahedrons which changes the electron distribution between Y^{3+} and oxygen ligands giving rise to two types of CTBs. Y_2O_3 is used as host for many rare earth dopants like Eu^{3+}, Tb^{3+}, Gd^{3+}, Dy^{3+}, Er^{3+}, Nd^{3+} and Sm^{3+} for applications in illumination, colour display, biomedical imaging and heavy ion dosimetry [**12-16**]. The co-doping of rare earth ions in Y_2O_3 (like Yb & Er and

Tm & Yb and so on) is used for upconversion phosphor application, fluorescence imaging etc. [17, 18]. The Er doped Y_2O_3 nano crystalline powder also shows upconversion green emission following excitation with low energy near infrared radiation (λ=980 nm) [19, 20]. The Yb doped Y_2O_3 (Yb: Y_2O_3) is a well-studied material for IR laser application (absorption at 940 and 976 nm; lasing action at 1030 and 1070 nm) [21, 22]. Above studies on rare earth doped Y_2O_3 shows the emission in visible region which is due to characteristic electronic transition of dopant elements. However, very few reports are available on PL studies of Yb: Y_2O_3 in visible region because of low integrated emission intensity due to transition from CTB to ground level. Two broad emission bands are observed at 368 and 533 nm in Yb: Y_2O_3 for excitation wavelength 215 nm at 10K which are associated with CT-$^2F_{7/2}$ and CT-$^2F_{5/2}$ transitions but there is no differentiation between the CTBs associated with C_2 and C_{3i} centers [23]. The electronic transition arises due to Yb^{3+} in different host materials are extensively studied by L. V. Pieterson [23] and the emission due to Yb^{2+} is extensively reported by Dorenbos [2]. The Yb^{3+} ion in Y_2O_3 occupies any of the two sites i. e. either C_2 or C_{3i} sites and hence modifies the electronic distribution in Y_2O_3 which in turn changes the energies of CTBs associated with C_2 and C_{3i} [24]. A clear picture on CTBs associated with C_2 and C_{3i} centers is still matter of investigation.

In the present work, the luminescence properties of nano Yb: Y_2O_3 was studied at different doping percentage of Yb. The dopant Yb is chosen because Yb^{3+} ions possess high quantum efficiency, relatively long fluorescence lifetime, wide absorption and emission bands and these ions were already demonstrated as a suitable active candidate for high intensity fluorescence [25-27]. Moreover, the effective ionic radius of Yb^{3+} is very close to Y^{3+} (Yb^{3+} (0.087 nm), Y^{3+} (0.09 nm)) which replace host lattice cation without changing crystal structure [28]. The aim of this work is to study the change in charge transfer band related luminescence in Yb doped Y_2O_3 due to near UV excitation (available LED). It is found that the excitation and emission wavelengths of nano Yb: Y_2O_3 are correlated using CTB associated with C_{3i} and C_2 sites. The energy level diagram of nano Yb: Y_2O_3 for visible emission is presented to explain broad emission in visible region. The luminiscence spectra of nano and bulk Yb: Y_2O_3 particles were compared with each other and also with bulk Y_2O_3. The possible use of Yb: Y_2O_3 nanoparticles have also been emphasized because of its broad emission in visible range.

Experimental

Materials synthesis

The Yb:Y_2O_3 nanoparticles were prepared by co-precipitation method [29]. High purity Y_2O_3 and Yb_2O_3 (Alfa Aesar make, 99.999% purity, product no: 11182) were used as starting materials. The steps involved in preparation of Yb: Y_2O_3 nanopowders from its salts are: (1) preparation of the Yb doped yttrium nitrate (mother solution), (2) addition of NH_4OH into mother solution till formation of $Y(OH)_3$ precipitate, (3) filtration and washing of precipitate with water, (4) drying and (5) calcinations of precursor powder. The dried Yb doped $Y(OH)_3$ precursor was calcined at 900 ºC to get nano powders of Yb: Y_2O_3. Using above procedure, Yb: Y_2O_3 nano powders were synthesized with 2, 5 and 8 mole percentage of Yb.

Characterization

The phase and crystallite size of powders calcined at 900 ºC were determined using X-ray diffractometer (Rigaku X-ray diffractometer with a Ni filtered Cu Kα radiation source and wavelength λ of the source being 1.54 Å). The size and morphology of nanoparticles were determined using transmission microscopy (TEM). Nanoparticles dissolved in chloroform are placed on the grid drop wise and the excess liquid is allowed to evaporate. The grids are examined in Philips CM200 electron microscope equipped with a tungsten cathode and operated at 200 kV. The photoluminescence (PL) measurement of nanoparticles was carried out at different absorption wavelength using PL spectrometer (FLS920-s, Edinburgh Instruments Ltd.) at room temperature. The background excitation source used for this purpose was a 450 W ozone-free Xenon arc lamp with continuous output. A calibrated photodiode and a R928P photomultiplier are used as excitation and emission detectors in visible range.

Results and discussion

The X-ray diffraction patterns of (2-8 mol %)Yb: Y_2O_3 nano powders are shown in **Fig. 1**.

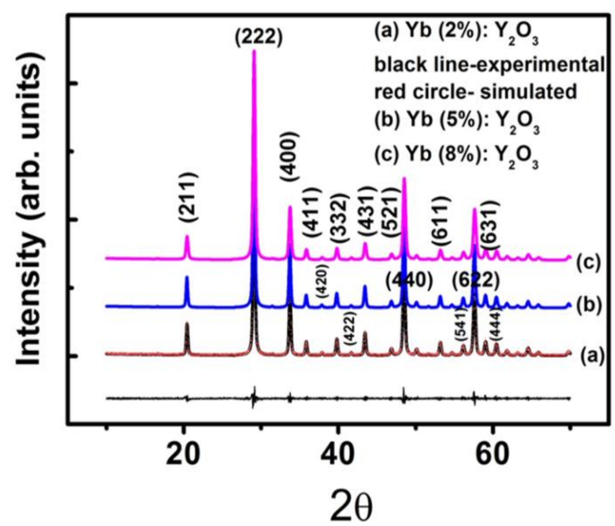

Fig. 1. X-ray diffraction pattern of the Yb: Y_2O_3 nanoparticles; (a) 2%Yb, (b) 5% Yb and (c) 8% Yb. In figure (a) the black line represents experimental, the red circle represents simulated and the difference line is shown below XRD patterns.

The XRD patterns were simulated and the calculated structural parameters are listed in **Table 1.** The structure of Yb: Y_2O_3 samples were found to be cubic (*Ia-3*) with slight change in their lattice parameter with no phase change compared to Y_2O_3 [**30**].

The lattice constants and the lattice volume were decreased with subsequent Yb doping due to smaller ionic radius of Yb^{3+} (0.087 nm) compared to ionic radius of Y^{3+} (0.09 nm) [**28**]. The lattice parameters of Yb doped Y_2O_3 nanopowders were also calculated using Vegard's law (by using lattice parameters of Y_2O_3 = 10.601; JCPDS No. 41-1105 and Yb_2O_3 = 10.43; JCPDS No.78-1690, 82-2417). The calculated lattice parameters for 2, 5 and 8 percentage Yb: Y_2O_3 are 10.597, 10.592 and 10.587 Å respectively which are well matched with experimental results. Debye Scherrer formula was utilized to determine the crystallite size (by substracting instrumental broadening from FWHM of peaks) of nano Yb:Y_2O_3. The average size of crystallites is found to be 45-70 nm **(Table 1)** and it is found that the crystallite size decreases with increasing Yb content.

The TEM bright field images of nanocrystalline (2-8 mol%) Yb: Y_2O_3 are shown in **Fig. 2**. The average particle size obtained from TEM micrographs for 2, 5 and 8mole% Yb:Y_2O_3 were 65-70 nm, 60-65 nm and 55-45 nm respectively. Particle size was found to decrease with increasing Yb mole percentage in Y_2O_3 and the morphology of the particles was almost remains same for all Yb: Y_2O_3 nanopowders.

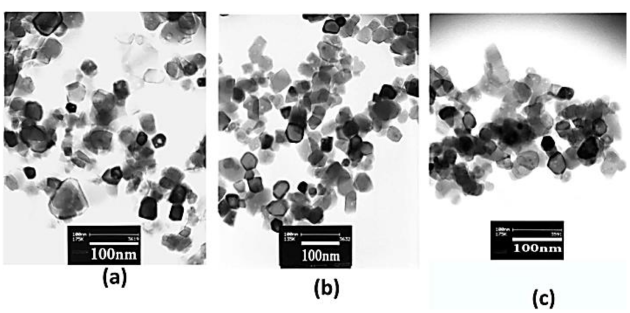

Fig. 2. Transmission electron microscopic images of Yb: Y_2O_3nano powders; (a) 2%Yb, (b) 5% Yb and (c) 8% Yb.

The excitation and emission spectra for 2, 5 and 8% Yb: Y_2O_3 nano powders are shown in **Fig. 3, 4** and **5** respectively. The excitation spectra for (2%) Yb: Y_2O_3 nano powder was recorded by keeping detector at 420 nm and two broad excitation peaks were observed at 335 nm and 370 nm **(Fig. 3(a)).**

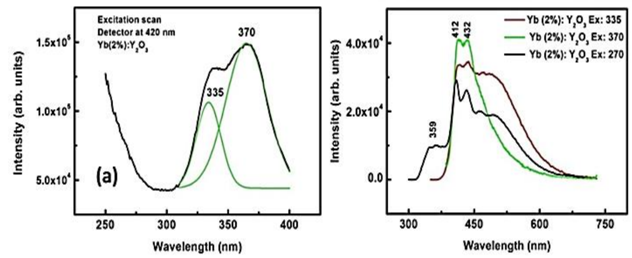

Fig. 3. Photoluminescent spectra of Yb(2%): Y_2O_3; (a) excitation spectra keeping detector at 420 nm and (b) emission spectra at excitation 335 nm (Red), 370 nm (green), 270 nm (black) and 420 nm (blue).

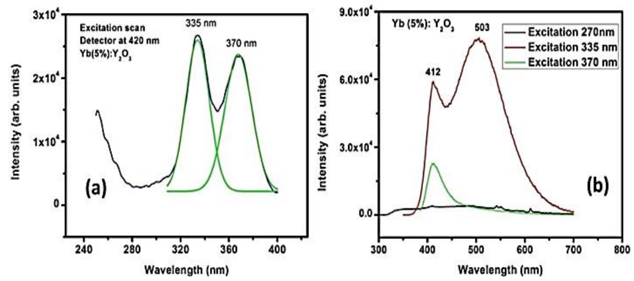

Fig. 4. Photoluminescent spectra of Yb(5%): Y_2O_3;(a) excitation spectra keeping detector at 420 nm and (b) emission spectra at excitation 335 nm (Red), 370 nm (green), 270 nm (black).

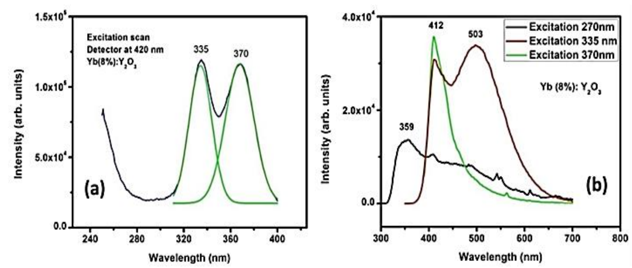

Fig. 5. Photoluminescent spectra of Yb(8%): Y_2O_3; (a) excitation spectra keeping detector at 420 nm and (b) emission spectra at excitation 335 nm (Red), 370 nm (green), 270 nm (black).

The peak at 370 nm is more intense compared to peak 335 nm for 2%Yb: Y_2O_3; however, intensity of the peak at 335 nm is more as compared to that at 370 nm (**Fig. 4a**) for 5%Yb: Y_2O_3. We have observed two excitation bands at 335 and 370 nm for 8% Yb: Y_2O_3 similar to 5%Yb: Y_2O_3 except the decrease in intensity of peak at 335 nm **(Fig. 5a)**. It confirms the existence of two strong

Table 1. Structural parameters and crystallite size for nano Yb (2, 5 and 8%): Y_2O_3.

Materials name	**Lattice Parameters**						**Space group**	**Volume of Unit Cell(A^3)**	**Crystallite size**
	a	**b**	**c**	**α**	**β**	**γ**			
Yb: Y_2O_3 (2%)	10.595	10.595	10.595	90	90	90	Ia-3	$1.1894*10^3$	69.966
Yb: Y_2O_3 (5%)	10.592	10.592	10.592	90	90	90	Ia-3	$1.1884*10^3$	67.370
Yb: Y_2O_3 (8%)	10.588	10.588	10.588	90	90	90	Ia-3	$1.1870*10^3$	46.745

bands in between valence and conduction band of Yb: Y_2O_3 from which transition of electron takes place at particular excitations i.e. 370 and 335 nm. In order to find the origin of these transitions in nano Yb: Y_2O_3 powder, the PL studies of pure Y_2O_3 (bulk powder) and Yb: Y_2O_3 (transparent ceramic pellet) were also carried out and are shown in **Fig. 6** and **Fig. 7** respectively. We observed only one broad peak (maximum at 324 nm) in the excitation spectra of bulk Y_2O_3 **(Fig. 6(a))** while for bulk Yb: Y_2O_3 two excitation peaks at 335 and 370 nm **(Fig. 7(a))** similar to that of nano Yb: Y_2O_3 powders. Therefore it is confirmed that the presence of 335 nm and 370 nm peaks in the excitation spectra of bulk and nano Yb: Y_2O_3 is due to Yb^{3+} dopant.

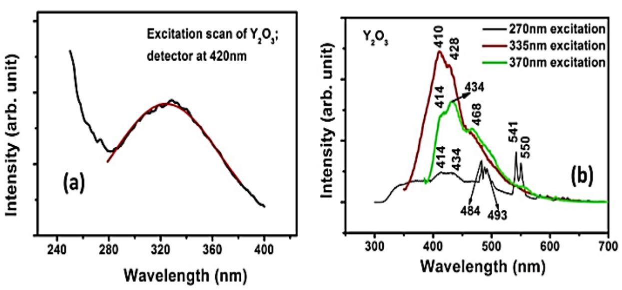

Fig. 6. Photoluminescent spectra of Y_2O_3 bulk powder (a) excitation spectra keeping detector at 420 nm and (b) emission spectra at excitation 335 nm (Red), 370 nm (green), 270 nm (black).

Fig. 3(b) shows the emission spectra of 2% Yb: Y_2O_3 excited at 270, 335 and 370 nm. Broad emission bands centered at ~359 nm, ~400 nm and ~503 nm were observed in emission spectrum of 2%Yb: Y_2O_3 for 270 nm excitation. The broad emission peak at ~503 nm is less intense compared to the peak at ~400 nm. The broad peak at ~400 nm splits into two sub peaks centered at 412 nm and 432 nm. When 2%Yb: Y_2O_3 nano powders are excited at 335 nm, the PL intensity of broad emission peaks i.e. at ~400 nm and ~503 nm was increased as compared to 270 nm excitation. The emission spectra of 5%Yb: Y_2O_3 excited at different wavelengths is shown in **Fig. 4(b)**.

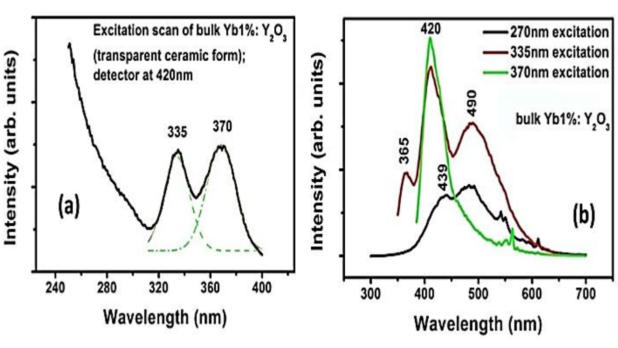

Fig. 7. Photoluminescent spectra of Yb(1%): Y_2O_3 bulk transparent ceramic (a) excitation spectra keeping detector at 420 nm and (b) emission spectra at excitation 335 nm (Red), 370 nm (green), 270 nm (black).

A broad emission band in the range from 335 nm to 600 nm was observed with less PL intensity (as compared to that of 2%Yb: Y_2O_3) for 270 nm excitation. The emission spectrum consists of two broad bands centred at ~412 and ~503 nm and extended in a range between ~390 nm to 600 nm for 335 nm excitation. The energy gap between two bands amounts to ~4500 cm^{-1} which is very less as compared to the energy difference between $^2F_{5/2}$ and $^2F_{7/2}$ of Yb^{3+}. The stoke shifts for ~412 and ~503 bands are 5460 and 9976 cm^{-1} respectively. The broad emission peak at ~412 nm appears for all excitation wave lengths; however, the broad peak at ~503 nm is absent for 370 nm excitation. **Fig. 5(b)** shows emission spectra of 8% Yb: Y_2O_3 at excitation wave lengths 270 nm, 335 nm and 370nm.

The spectrum is similar to that of 5%Yb: Y_2O_3 except the decrease in integrated emission peak intensity. The decrease in PL intensity for 8%Yb: Y_2O_3 compared to 5%Yb: Y_2O_3 may be explained on the basis of creation of more defect states due to smaller ionic radius of Yb which leads to decrease in the lattice parameters. Since more defect states are created for 8%Yb: Y_2O_3 which may lead to high non-radiative relaxation [**31**]; hence decrease in PL intensity as compared to 5%Yb: Y_2O_3. It is also reported that the decrease in crystallite size reduces the PL intensity in rare earth doped Y_2O_3 [**32**]. The crystallites in 8%Yb: Y_2O_3 are very small as compared to that of 5%Yb: Y_2O_3. This may be one of the cause of decrease in PL intensity. In addition to broad peaks, very small peaks at 483,488, 493, 541, 555 and 612 nm are present in PL spectra of Yb: Y_2O_3 for 270 nm excitation. Small intensity peaks observed at 483, 488, 493 and 612 nm are attributed to the presence of Yb in Y_2O_3 [**33**].

The emission spectrum of bulk Y_2O_3 and Yb: Y_2O_3 are shown in **Fig. 6(b)** and **7(b)** respectively. In bulk Y_2O_3 we observed two broad emission peaks at ~410 nm and ~468 nm for both 335 and 370 nm excitations. In bulk Yb: Y_2O_3 two broad peaks at ~420 nm and ~490 nm was also observed for 335 nm excitation; however, one broad emission peak at 420 nm was observed for 370 nm excitation. The presence of high intense broad peak at ~ (410 – 440 nm) in all the samples with or without Yb doping and in bulk as well as in nano form of Yb: Y_2O_3 confirms that this band is associated with stable CTB due to non centrosymmetric C_2 sites. The peak position of this band is slightly changed due to Yb doping in Y_2O_3 as compared to pure Y_2O_3.

The broad emission peak observed at ~503 nm for nano Yb: Y_2O_3 and emission peak at ~490 nm for bulk Yb: Y_2O_3 may correspond to a CTB and its position depends on the doping percentage of Yb in Y_2O_3. Therefore, this CTB may be assigned to centrosymmetric C_{3i} centres whose appearance depends on size of particles and percentage of dopant in the matrix. In Y_2O_3 the intensity of peak due to CTB associated C_{3i} centers is very less as compared to the intensity of peak associated with C_2 centers which may be attributed to very small distortion of centrosymmetricity of C_{3i} centres. In bulk Yb: Y_2O_3 the emission peak associated with distorted C_{3i} centres are shifted towards higher wave lengths as compared to Y_2O_3 and the intensity becomes prominent due to creation of more distortion at C_{3i} sites due to Yb doping. In case of nano Yb: Y_2O_3 further distortions occur at C_{3i} sites to break centrosymmetry and more transitions are allowed so as to observe intense emission at ~503 nm. The emission band at ~503 nm mainly appears for 335 nm or small wave length excitation made it clear that the CTB associated with C_{3i} centers must have higher energy compared to the CTB associated with C_2 centers. From the above discussion, it is confirmed that two types of CTBs associated with C_2 and C_{3i} symmetry centers of Y_2O_3 are present in Yb: Y_2O_3. The position of CTB associated with C_{3i} depends on type of dopant, percentage of dopant and size of the particles etc. These two charge transfer states correspond to ligand interactions at two different Y^{3+} positions in nano Y_2O_3 [**16**]. The separation between two CTBs is around 2823 cm^{-1}.

Small intensity peaks are also observed in bulk Y_2O_3 (as purchased micron size powder; Alfa Aesar; product no 11182) and bulk Yb: Y_2O_3 at 483,488, 493 and 612 nm for above band gap excitation i. e. 270 nm. These are attributed to the presence of Yb in the bulk material [**34**].

The characteristic peaks at 541 and 555 nm confirms the presence of Er impurity in the bulk Y_2O_3. Since nano powders of Yb:Y_2O_3 are prepared using these Y_2O_3 powders, small extra characteristic peaks of Er are also present in the PL spectra of Yb:Y_2O_3.

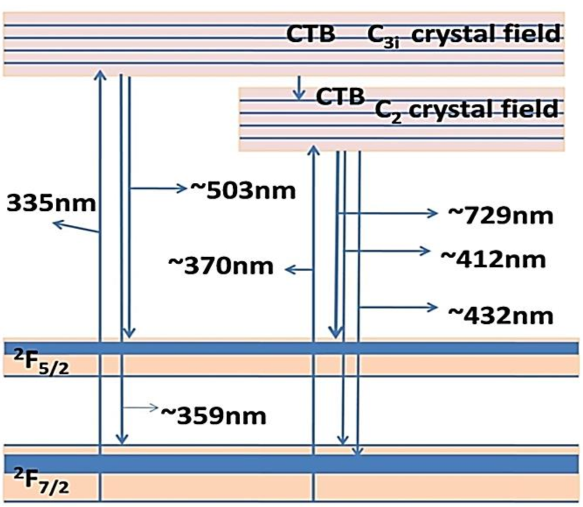

Fig. 8. Schematic energy level model of Yb: Y_2O_3 nano phosphor.

The observed excitation and emission spectra has been summarized in the energy level diagram as shown in **Fig.8**. The electronic transitions occur between CTB (associated with C_2 and C_{3i} centres of host Y_2O_3) and ground level ($^2F_{5/2}$ and $^2F_{7/2}$ created due to Yb doping). Here it worth to note that the 4f-4f transition and CTB-4f are two different types of transitions of the Yb^{3+} ions in crystals. The 4f orbital is shielded from the surrounding by the filled $5s^2$ and $5p^6$ orbital. Therefore, the influence of host lattice on the optical transitions within the $4f^n$ configuration is small and 4f-4f transitions occur in IR region, while the CTB absorption shows a broad band character and intense than that of 4f-4f transition and lies in visible region.

The excitation peak at 370 nm corresponds to transition of electron from ground level ($^2F_{7/2}$) to CTB associated with C_2 charge centre and the peak at 335 nm corresponds to excitation of electron to CTB associated with C_{3i} charge centre from $^2F_{7/2}$ level because the absorption energy level of C_{3i} centers is at higher energy than that of the C_2 centers.[34]The intensity of 335nm peak in excitation spectra depends on doping percentage of Yb in Y_2O_3 because this transition depends on the number of C_{3i} charge centres at which there is broken of centre of symmetry (i. e. for 2% Yb doped Y_2O_3 nano powder the number of C_{3i} centres for which the centrosymmetricity was broken is less compared to 5% and 8% Yb doped Y_2O_3 nano powders).

The possible broad emission peaks ~359 nm, ~400 nm (centered at 412 nm &430 nm) and ~503 nm observed for 270 nm excitation correspond to CTB (C_{3i}) - $^2F_{7/2}$, CTB (C_2) - $^2F_{7/2}$ and CTB (C_{3i}) - $^2F_{5/2}$ (~503nm) transitions respectively. According to the energy level diagram, for 335 nm excitation (i. e. from $^2F_{7/2}$ to CTB (C_{3i})) the possible strong emission bands at ~503 nm, 412 nm, 359 nm and 729 nm are due to CTB (C_{3i}) - $^2F_{5/2}$, CTB (C_2) - $^2F_{7/2}$, CTB (C_{3i}) - $^2F_{7/2}$ and CTB (C_2) - $^2F_{5/2}$transition respectively. The peak at 729 nm was not observed in PL spectra due to limitation of PL scan range (to avoid 1st and 2nd order excitation diffraction peak). Similarly, for 370 nm excitation the strong possible broad emission peak was observed at ~412 nm due to electron transition from CTB (C_2) to $^2F_{7/2}$. From above discussion, it is understood that due to activation of centrosymmetric (C_{3i}) sites in nano Yb: Y_2O_3 powders strong broad PL in the range from ~400 to ~ 650 nm is observed.

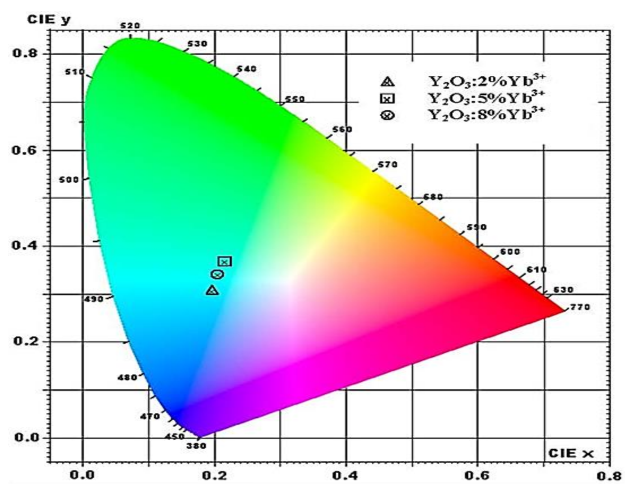

Fig. 9. The color coordinate diagram for Y_2O_3:Yb^{3+} nanophosphors for different Yb^{3+} concentration.

The CIE (International Commission on Illumination) chromaticity illustration of Y_2O_3:Yb^{3+} nanophosphor for various molar concentration of Yb^{3+} is shown in **Fig. 9**. From the chromaticity diagram (**Fig. 9**), it can be seen that colour coordinates transverse from bluish white to greenish white region with increase in Yb^{3+} doping concentration. The CIE colour coordinates (x, y) are shown in **Table 2**.

The CIE parameter colour purity of emitted colour is useful for narrow banded light sources and for broad band light sources CCT (Correlated Color Temperature) is more useful [**35**]. The CCT were calculated by the McCamy empirical formula and are summarized in **Table 2**; [**36**, **37**]

$$CCT = - 437n^3 + 360n^2 - 6861n + 5514.31 \quad (1)$$

where, $n = (x-x_e)/(y-y_e)$ and chromaticity epicenter is at $x_e = 0.3320$ and $y_e = 0.1858$. The CCT values shows the color temperatures correspond to bluish white for Yb: Y_2O_3 nanophosphors.

Table 2. Photometric parameters of nano Yb (2, 5 and 8%): Y_2O_3.

Nano-phosphor	Concentration (mol%)	Colour Coordinates x	Colour Coordinates y	CCT (K)
Y_2O_3:Yb^{3+}	2	0.195	0.304	18984.603
	5	0.215	0.365	11650.510
	8	0.206	0.339	13836.115

Conclusion

In the present work, we have investigated the photoluminescence properties of nano Yb: Y_2O_3 with different doping percentage of Yb in visible region. The nano Yb: Y_2O_3 shows intense and broad excitation peaks at 335 nm and 370 nm. The excitation peak at 370 nm is obvious due to transition of electrons from $^2F_{7/2}$ to CTB associated with non-centrosymmetric C_2 centers but the excitation peak at 335 nm is due to transition of electrons from $^2F_{7/2}$ to the CTB associated with distorted centrosymmetric C_{3i} centers. A broad intense emission peak observed at ~503 nm is assigned to transition from CTB (C_{3i}) to $^2F_{5/2}$ energy levels. The Yb doping in Y_2O_3 not only modify the charge transfer bands but also provides ground energy levels to the emitted electron which results in strong intense broad emission ranging from ~400 to ~650 nm. Among various doping percentage of Yb in Y_2O_3, the 5%Yb doped Y_2O_3 nano phosphor shows high integrated emission intensity at ~503 nm for ~335 nm excitation. Therefore by using AlGaN based LED (output peak at ~335 nm with FWHM 10 nm, commercially available) the 5%Yb: Y_2O_3 nano phosphor may use to produce bluish white light.

Acknowledgements

Authors are grateful to Mr. Himanshu Srivastava, ISUD, RRCAT, Indore for TEM of nanoparticles. We are also thankful to Mr. Gopal Mohod, for his help in infrastructure development for experimental setups.

Author's contributions

All have equal contribution. Authors have no competing financial interests.

References

1. Rydberg, S. and Engholm, M.; *J. Appl. Phys.* **2013,** *113*, 223510. **DOI:** 10.1063/1.4810858
2. Dorenbos, P.; *J. Phys. Condens Matter* **2003**, *15*, 8417. **DOI:** 10.1088/0953-8984/15/49/018
3. Yanmin, Q.; Xinbo, Z.; Xiao, Y. E.; Yan, C.; Hai, G. *J. Rare earths* **2009**, *27*, 323. **DOI:** 10.1016/S1002-0721(08)60243-4
4. Park, J. K.; Choi, K. J.; Kim, K. N. and Kim, C. H. *Appl. Phys. Lett.* **2005**, *87*, 031108. **DOI**: 10.1063/1.1984103
5. Park, J. K.; Kim, C. H.; Park, S. H. and Park, H. D. *Appl. Phys. Lett.* **2004,** *84*, 1647. **DOI:** 10.1063/1.1667620
6. Hiramatsu, R.; Ishida, K.; Aiga, F.; Fukuda, Y.; Matsuda, N. and Asai, H. *J. Appl. Phys.* **2009**, *106* , 093513. **DOI:** 10.1063/1.3253721
7. Nigara, Y. *Jpn. J. Appl. Phys.***1968,** *7*, 404. **DOI**: 10.1143/JJAP.7.404
8. Tiwari, A., *Advanced Materials Letters*, **2012**, 3.
9. Fukabori, A.; Yanagida, T.; Pejchal, J.; Maeo, S.; Yokota, Y.; Yoshikawa, A.et al. *J. Appl. Phys.* **2010**,*107*,073501. **DOI:** 10.1063/1.3330407
10. Tarner, P. A.; Duan, C. –K. *Coord. Chem. Rev.* **2010**, *254*, 3026. **DOI:** 10.1016/j.ccr.2010.05.009
11. Vetrone, F.; Boyer, J-C. and Capobianco, J. A. Yittrium Oxide nano crystals: Luminescent properties and Applications, Encyclopedia of Nano science and Nano technology, Nalwa, H. S. (Ed) American Scientific publisher **2004**, 10, 725.
12. Som, S.; Dutta, S.; Chowdhury, M.; Kumar, V.; Kumar, V.; Swart, H. C.; Sharma, S. K. J. *Alloys. Comp.*, **2014**, *589*, 5. **DOI:** 10.1016/j.jallcom.2013.11.182
13. Kodaira, C. A.; Stefani, R.; Maia, A. S.; Felinto, M. C. F. C. and Brito, H. F. *J. Luminescence* **2007,** *127* , 616. **DOI:** 10.1016/j.jlumin.2007.03.016
14. Vitrone, F.; Boyer, J. C.; Capobianco, J. A.; Speghini, A. and Bettinelli, M. *Nanotechnology* **2004**, *15* , 75. **DOI:** 10.1088/0957-4484/15/1/015
15. Loitongbam, R. S.; Singh, W. R.; Phaomei, G. and Singh, N. S. *Journal of Luminescence* **2013,** *140*,95. **DOI:** 10.1016/j.jlumin.2013.02.049
16. Ju, G.; Hu, Y.; Chen, L.; Wang, X.; Mu, Z.; Wu, H. and Kang, F. *Journal of Luminescence* **2012**, *132*, 1853. **DOI:** 10.1016/j.jlumin.2012.03.020
17. Hou, X.; Zhou, S.; Lin, H.; Teng, H.; Li, Y. and Jia, T. *J. appl. Phys.* **2010**, *107*, 083101. **DOI:** 10.1063/1.3380820
18. Vetrone, F.; Boyer, J. C.; Capobianco, J. A.; Speghini, A. and Bettinelli, M. *J. Appl. Phys.* **2004**, *96*, 661. **DOI:** 10.1063/1.1739523
19. Vitrone, F.; Boyer, J. C.; Capobianco, J. A.; Speghini, A. and Bettinelli, M. *Chem. Mater*. **2003**, *15* 2737. **DOI:** 10.1021/cm0301930
20. Vitrone, F.; Boyer, J. C.; Capobianco, J. A.; Speghini, A. and Bettinelli, M. *J. Phys. Chem. B* **2002**, *106*,1181. **DOI:** 10.1021/jp0129582
21. Takaichi, K.; Yagi, H.; Lu, J.; Bisson, J. F.; Shirakawa, A.; Ueda, K.; Yanagitani, T.; Kaminskii, A. A. *Appl. Phys. Lett.* **2004**, *84*, 317. **DOI**: 10.1063/1.1641514
22. Kong, J.; Tang, D. Y.; Lu, J. and Ueda, K. *Appl. Phys. B* **2004**, *79*, 449. **DOI:** 10.1007/s00340-004-1594-3
23. Van Pieterson, L.; Heeroma, M.; De Heer E.; Meijerink, A. *J. Lumin.* **2000**, *91*, 177. **DOI:** 10.1016/S0022-2313(00)00214-**3**
24. Krasikov, D. N.; Scherbinin, A. V.; Vasilev, A. N.; Kamenskikh, I. A.; Mikhailin, V. V. *J. Lumin.* **2008**, *128*, 1748. **DOI:** 10.1016/j.jlumin.2008.04.001
25. Krupke, W. F. *IEEE J. Sel. Top. Quant. Electron.***2000**, *6*, 1287. **DOI:** 10.1109/2944.902180
26. Chenais, S.; Druon, F.; Forget, S.; Balembois,F.; Georges, P. *Prog. Quant. Electron*, **2006,** *30*, 89.

DOI: 10.1016/j.pquantelec.2006.12.001

27. Matsushima, I.; Tanabashi, A. *Opt. Rev.* **2010**, *17*, 294.
28. Shannon, R. D. *Acta Cryst. A* **1976**, *32*, 751.
DOI: 10.1107/S0567739476001551
29. Satapathy, S.; Ahlawat, A.; Paliwal, A.; Singh, R.; Singh, M. K. and Gupta, P. K. *CrystEngComm.* **2014**, *16*, 2723.
DOI: 10.1039/C3CE42529K
30. Huang, Z.; Sun, X.; Xiu, Z.; Chen, S. and Tsai, C. *Materials Lett.* **2004**, *58*, 2137.
DOI: 10.1016/j.matlet.2004.02.008
31. Gorge, A.; Sharma, S. K.; Chawla, S.; Malik, M. M. and Qureshi, M. S. *J. Alloys. Compd.* **2011**, *509*, 5942.
DOI: 10.1016/j.jallcom.2011.03.017
32. Wang, W. N.; Widiyastuti, W.; Ogi, T.; Lenggoro, I. W. and Okuyama, K. *Chem. Mater*. **2007,** *19*, 1723.
DOI: 10.1021/cm062887p
33. Agrawal, S. and Dubey, V. *J. Radiation Research and Applied Sciences* **2014**, *7*, 601.
DOI: 10.1016/j.jrras.2014.09.014
34. Boulon, G. and Lupei, V. *J. Lumin.* **2007**, *125*, 45.
DOI: 10.1016/j.jlumin.2006.08.056
35. Som, S.; Kunti, S.; Kumar, V.; Kumar, V.; Dutta, S.; Chowdhury, M.; Sharma, S. K.; Terblans, J. J. and Swart, H. C. *J. Appl. Phys.***2014**, *115*, 193101.
DOI: 10.1063/1.4876316
36. McCamy, C. S. *Color Res Appl*. 1992, *17*,142;
DOI: 10.1002/col.5080170211
37. Som, S.; Mitra, P.; Kumar, V.; Kumar, V.; Terblans, J. J.; Swart, H. C. and Sharma, S. K. *Dalton Trans.***2014**,*43*, 9860.
DOI: 10.1039/C4DT00349G